Eur. Phys. J. A **27**, 213–223 (2006)
DOI 10.1140/epja/i2005-10246-4

THE EUROPEAN PHYSICAL JOURNAL A

Electromagnetic structure and weak decay of pseudoscalar mesons in a light-front QCD-inspired model

L.A.M. Salcedo[1,a], J.P.B.C. de Melo[2,3,b], D. Hadjimichef[4], and T. Frederico[1]

[1] Departamento de Física, Instituto Tecnológico de Aeronáutica, Cento Técnico Aeroespacial, 12.228-900 São José dos Campos, São Paulo, Brazil
[2] Centro de Ciências Exatas e Tecnológicas, Universidade Cruzeiro do Sul, 08060-070, São Paulo, Brazil
[3] Instituto de Física Teórica, Universidade Estadual Paulista, 01405-900, São Paulo, Brazil
[4] Instituto de Física e Matemática, Universidade Federal de Pelotas, 96010-900, Campus Universitário Pelotas, Rio Grande do Sul, Brazil

Received: 19 September 2005 / Revised version: 11 February 2006 /
Published online: 14 March 2006 –
Communicated by V. Vento

Abstract. We study the scaling of the $^3S_1$-$^1S_0$ meson mass splitting and the pseudoscalar weak-decay constants with the mass of the meson, as seen in the available experimental data. We use an effective light-front QCD-inspired dynamical model regulated at short distances to describe the valence component of the pseudoscalar mesons. The experimentally known values of the mass splitting, decay constants (from global lattice-QCD averages) and the pion charge form factor up to 4 $[\mathrm{GeV}/c]^2$ are reasonably described by the model.

PACS. 12.39.Ki Relativistic quark model – 13.20.-v Leptonic, semileptonic, and radiative decays of mesons – 14.40.-n Mesons

1 Introduction

The structure of light-front hadronic wave functions in terms of constituent quarks has been investigated since it were first formulated in 1976 [1,2], when still Quantum Chromodynamics was in its infancy. After these seminal works, light-front phenomenology has been turned into a lively field of research (see, for instance, the recent review [3]).

One important aspect in the light-front phenomenology is the hadronic structure viewed through effective theories inspired by Quantum Chromodynamics [3–8]. This can shed light on the investigation of the interaction between the hadron constituents and on the study of the transition from effective to fundamental degrees of freedom, that should be revealed at large momentum scales.

The effective light-front QCD model is expressed through a square mass operator acting on the valence component of the hadron wave function. The effective interaction embeds, in principle, all the complexity of QCD through the coupling of the valence state with higher Fock states, reduced to the valence sector [7]. The effective square mass operator depends on few physical parameters: the constituent-quark masses, the effective quark-gluon coupling entering in the Coulomb-like interaction and the strength of the short-range hyperfine interaction, fixed by the pion mass [8].

Let us discuss the relation of the model to QCD. The basic aspect of QCD beyond the general features of quark degrees of freedom is the coupling between the $|q\overline{q}\rangle$ and the three-particle $|q\overline{q}g\rangle$ Fock component of the wave function which has one gluon and a quark-antiquark pair and gives rise to the one-gluon exchange interaction. The Fock space coupled-channel eigenvalue equation for the square mass operator written in a compact form is $\mathcal{M}^2|\Psi\rangle = M_h^2|\Psi\rangle$, where schematically $|\Psi\rangle = |\psi_{q\overline{q}}\rangle + |\psi_{q\overline{q}g}\rangle + \cdots$ is the decomposition of the meson wave function in Fock components. The projection operator on the valence sector is P ($P|\Psi\rangle = |\psi_{q\overline{q}}\rangle$) and $Q = 1 - P$. The reduction of the square mass eigenvalue equation to the valence sector is given by

$$\left[P\mathcal{M}^2P + P\mathcal{M}^2Q\frac{1}{M_h^2 - \mathcal{M}^2}Q\mathcal{M}^2P\right]|\psi_{q\overline{q}}\rangle = M_h^2|\psi_{q\overline{q}}\rangle, \tag{1}$$

where one identifies the effective interaction as the second term in the right-hand side of the above equation.

[a] *Present address*: Instituto de Física, Universidade Federal do Rio Grande do Sul, Campus do Vale, 91501-970 Porto Alegre, Rio Grande do Sul, Brazil.
[b] e-mail: pacheco@ift.unesp.br

The first term in a Fock expansion of the resolvent in the effective interaction corresponds to the truncation of the Q-space at the gluon-quark-antiquark sector, which corresponds to the one-gluon exchange contribution. However, the resolvent in eq. (1) couples the valence sector to all Fock components (see refs. [3] and [28]), and in our simplified model all this complex physics comes through the effective quark-gluon coupling constant and the hyperfine interaction parameters.

Hadronic observables are functions of these parameters and quark masses. A physically sensible model dependence is on the quark masses, which allows to get insight into the limit of heavy quarks. In particular, this limit is reflected in the weak-decay constant of pseudoscalar heavy-light mesons, which in potential models were found to be $\propto 1/\sqrt{m_Q}$ [9] (m_Q is the heavy quark mass). Also, this scaling property has been shown in a light-front constituent-quark model [10]. (We do not intend to be complete in our references.)

The weak-decay constant is closely related to the physics at small distances contained in the valence component of the pseudoscalar meson light-front wave function. It constitutes an important source of information on the short-range part of the quark-antiquark interaction. Experimental values for the weak-decay constants are known for the pion, kaon, D^+ and D_s^+ [11]. The dependence of the effective theory in their few parameters can be translated into correlations between observables of a particular hadron or among different hadrons. Therefore, it is possible to indicate relevant relations between physical quantities that otherwise would have no simple reason to exhibit a close dependence, besides being properties of the same basic theory. For example, in the recent review [12] of the application of Dyson-Schwinger equations to QCD, systematic correlations between different meson properties with mass scales were shown, which were also useful to compare the pseudoscalar decay constants with results from Lattice QCD.

The experimental values of the mass splitting between the ground states of pseudoscalars and vector mesons present a systematic dependence with the corresponding pseudoscalar mass, which is well described by the effective QCD theory even without confinement [8]. The mass splitting is associated with the binding energy of the quark-antiquark pair in the meson, as that model lack a confining interaction. (It is worthwhile to note that the model account for the binding energy of the spin-1/2 ground-state baryons containing two light and one heavy quarks [13]).

In ref. [14] it was pointed out that f_{ps} should scale with the sum of the constituent-quark masses, and more recently in the context of a light-front QCD-inspired model it was found that f_{ps} scales with the vector meson mass [15]. In the light-front QCD-inspired model, without a short-range regulator, the dominance of the asymptotic wave function [15] was assumed. Both frameworks assume that the log-type singularity in the matrix element of the axial current between the vacuum and the meson state is fixed by the pion decay constant f_π. In these approaches, the weak-decay constant depends directly on the constituent masses and on the short-distance component of the valence part of the light-front meson wave function which is parameterized by f_π. Although the experimental results for light mesons up to D [11] suggest such an increase, relativistic constituent-quark models in the heavy-quark limit (see refs. [9,10]) and numerical simulations with quenched lattice-QCD [16] indicate that $f_D > f_B$ [16]. This is still maintained with two flavor sea quarks [16,17] and in the most recent global average of lattice results [18]. This behavior of the weak-decay constants of the heavy-light pseudoscalars is also found in a Dyson-Schwinger formalism applied to QCD, where general arguments say that in the heavy quark limit f_{ps} should be $\propto 1/\sqrt{M_{ps}}$ [19] (M_{ps} is the pseudoscalar mass). In order to study the mass dependence of the weak-decay constant we can attempt to use a regulated form of the light-front constituent-quark QCD-inspired model [5,6,8]. In this case, the systematical investigation of the mass dependence of meson observables can be easily performed as the masses of constituent quarks act as model parameters, which can be varied while the effective quark-gluon coupling entering in the Coulomb-like interaction is flavor independent.

The short-distance interaction between the constituent quarks in the square mass operator equation of the effective light-front QCD theory [8], if regulated, allows a finite result for the decay constant and electromagnetic form factor. In this case, the eigenstate of the effective mass operator, *i.e.*, the valence component of the light-front wave function, would decrease faster than $p_\perp^{-2}$ for large transverse momentum, which is enough to make finite the one-loop integration in the weak-decay constant and form factor. One can get some information on the short-distance behavior of the valence component of the pseudoscalar meson from the electromagnetic form factor, which is experimentally well known for the pion (see ref. [20]), while for the kaon data exists below $0.15\,(\mathrm{GeV}/c)^2$ [21,22]. In particular, when the asymptotic wave function is assumed for the soft-pion limit, its radius and decay constant are related by $\sqrt{\langle r_\pi^2\rangle} = \sqrt{3}/(2\pi f_\pi)$ [23–25].

Our aim in this work is to study systematically the mass dependence of the pseudoscalar weak-decay constant, the electromagnetic form factor and the mass splitting between the ground states of pseudoscalar and vector mesons, using a light-front QCD-inspired model regulated at short distances. We choose the regulator in a separable form to simplify the formalism. The effective mass operator equation for the valence component of a constituent quark-antiquark bound system was derived in the effective one-gluon exchange interaction approximation [3] and simplified in refs. [5,6]. The square mass operator includes a Coulomb-like and a Dirac-delta hyperfine interaction acting on the spin singlet state responsible for the mass separation between pseudoscalar and the vector meson states. Here, we extend the model by introducing a regulator in a separable form in the singular part of the interaction. Then, the eigenvalue equation for the effective

square mass operator is written as

$$M_{ps}^2\psi(x,\vec{k}_\perp) = M_0^2\psi(x,\vec{k}_\perp) - \int \frac{\mathrm{d}x'\mathrm{d}\vec{k'}_\perp\theta(x')\theta(1-x')}{\sqrt{x(1-x)x'(1-x')}} \times \left(\frac{4m_1m_2}{3\pi^2}\frac{\alpha}{Q^2} - \lambda g(M_0^2)g(M_0'^2)\right)\psi(x',\vec{k'}_\perp), \quad (2)$$

m_1 and m_2 are the constituent-quark masses. We have omitted the subindex $q\overline{q}$ of $|\psi\rangle$. The free square mass operator in the meson rest frame is

$$M_0^2 = \frac{\vec{k}_\perp^2 + m_1^2}{x} + \frac{\vec{k}_\perp^2 + m_2^2}{1-x}\,; \quad (3)$$

and $M_0'^2$ has primed momentum arguments. The form factor of the separable regulator function is $g(M_0^2)$. The mean four-momentum transfer is Q^2, which is approximated by a rotationally invariant form $Q^2 = |\vec{k} - \vec{k}'|^2$. The strength of the Coulomb-like potential is proportional to α and the coupling constant of the regulated Dirac-delta hyperfine interaction is given by λ. Note that for $g(M_0^2) \equiv 1$, the original unregulated form of the model presented in refs. [5,6] is retrieved. (In refs. [5] and [26] a local Yukawa potential for the regularization of the contact interaction was used, here we use a separable form for simplicity.)

The dependence of the form factor in terms of M_0^2 appears to be natural in a light-front theory, in which the virtuality of an intermediate state is measured by the value of the corresponding free square mass. In the rest frame of the quark-antiquark pair $M_0^2 = P_0^-\,P^+$ and therefore proportional to the free value of P_0^- —the minus component of the free momentum ($P_0^\pm = P_0^0 \pm P_0^3$).

Although a more developed form of the model is known which contains the explicit confinement [27], we will be content with solving eq. (2) which is enough for our purpose of studying only the ground state. In practice, from the solution of eq. (2), the constituents quarks are bound and, in that sense, confined in the interior of the mesons [8].

The present light-front model is a drastic approximation to a severe truncation of the Fock space in the effective theory. In the initial truncation of QCD only one-gluon exchange was kept, which includes Fock states with up to $q\overline{q}$ plus one gluon, leaving out the complex nonlinear structure of QCD [3,7] which appears only through the model parameters. The spin dependence and momentum dependence in the hyperfine interaction are greatly simplified to get eq. (2) (with $g(M^2) = 1$) and confinement is absent in the model. Therefore, the success of the model should be understood as a useful guide in the investigation of mesonic properties which present a systematic behavior that depends only on few basic quantities that are parameterized in the effective theory.

This work is organized as follows. In sect. 2 the QCD-inspired model is transformed into the instant form representation and the eigenvalue equation for the square mass operator is solved. The valence component of the meson wave function is derived. In sect. 3 we give the formulae for the electromagnetic form factor and weak-decay constant derived from an effective pseudoscalar Lagrangian used to construct the spin part of the pseudoscalar meson wave function. In sect. 4 we present and discuss the results obtained with the regularized model for the mass splitting between the pseudoscalar and vector mesons, the weak-decay constants and the pion and kaon form factors. Also, in sect. 4 we summarize our conclusions.

2 The QCD-inspired model in instant form representation

The effective square mass operator equation for the lowest light-front Fock state component of a bound system of a constituent quark and antiquark is rewritten in terms of the instant form momentum. Here we follow closely ref. [8]. The general transformation from the light-cone momentum to three-momentum was derived in ref. [4]. The form of eq. (2) in the instant form momentum basis is particularly simple and convenient for the numerical solution when the momentum carried by the effective gluon is approximated by a rotational invariant form. The momentum fraction is transformed into

$$x(k_z) = \frac{(E_1 + k_z)}{E_1 + E_2}\,, \quad (4)$$

with $\vec{k}_\perp$ unchanged. The individual energies are $E_i = \sqrt{m_i^2 + k^2}$ $(i = 1,2)$ and $k \equiv |\vec{k}|$. The Jacobian of the transformation $(x,\vec{k}_\perp)$ to $\vec{k}$ is

$$\mathrm{d}x\mathrm{d}\vec{k}_\perp = \frac{x(1-x)}{m_r A(k)}\mathrm{d}\vec{k}, \quad (5)$$

where the dimensionless phase-space function is given by

$$A(k) = \frac{1}{m_r}\frac{E_1E_2}{E_1+E_2} \quad (6)$$

and the reduced mass is $m_r = m_1m_2/(m_1+m_2)$.

Using the momentum transformation defined above, the eigenvalue equation (2), written in the instant form momentum basis, is

$$M_{ps}^2\varphi(\vec{k}) = M_0^2\varphi(\vec{k}) - \int \mathrm{d}\vec{k}'\left(\frac{4m_s}{3\pi^2}\frac{\alpha}{\sqrt{A(k)A(k')}Q^2} - \frac{\lambda\; g(M_0^2)\; g(M_0'^2)}{m_r\sqrt{A(k)A(k')}}\right)\varphi(\vec{k}'), \quad (7)$$

where $m_s = m_1 + m_2$, $M_0 = E_1 + E_2$ and M_0' has the primed momentum arguments. The phase-space factor is included in the factor $1/\sqrt{A(k)A(k')}$.

The valence component of the light-front wave function is

$$\psi(x,\vec{k}_\perp) = \sqrt{\frac{A(k)}{x(1-x)}}\varphi(\vec{k}). \quad (8)$$

The higher Fock state components of the light-front wave function of the composite system can be expressed in

terms of the lower ones, as shown by the method of the iterated resolvents [6] (presented in greater detail in [7]) and by a quasi-potential expansion on the light-front of the Bethe-Salpeter equation [28]. Therefore, it is possible to reconstruct recursively all the Fock state components of the wave function from the valence component. In this way, the full complexity of a quantum field theory can in principle be described by a light-front effective Hamiltonian acting in the lowest Fock state component of a composite system.

2.1 Meson valence wave function

To easily manipulate and solve eq. (7), it is convenient to work with the operator representation

$$\left(M_0^2 + V + V^\delta\right)|\varphi\rangle = M^2|\varphi\rangle. \tag{9}$$

The matrix elements of the Coulomb-like potential V are given by

$$\langle\vec{k}|V|\vec{k'}\rangle = -\frac{4m_s}{3\pi^2}\frac{\alpha}{\sqrt{A(k)}Q^2\sqrt{A(k')}}, \tag{10}$$

and for the short-range regularized singular interaction one has

$$\langle\vec{k}|V^\delta|\vec{k'}\rangle = \langle\vec{k}|\chi\rangle\frac{\lambda}{m_r}\langle\chi|\vec{k'}\rangle = \frac{\lambda}{m_r}\frac{g(M_0^2)}{\sqrt{A(k)}}\frac{g(M_0'^2)}{\sqrt{A(k')}}. \tag{11}$$

Just for convenience we kept the same superscript δ in the short-range part of the interaction as in ref. [8], although it is regulated here. We introduce a form factor defined by $\langle\vec{k}|\chi\rangle = g(M_0^2)/\sqrt{A(k)}$, which now includes the regulator.

The eigenstate of the square mass operator (9) is trivially given by

$$|\varphi\rangle = G^V(M_{ps}^2)|\chi\rangle, \tag{12}$$

where $G^V(M_{ps}^2) = \left[M_{ps}^2 - M_0^2 - V\right]^{-1}$ is the resolvent of the operator $M_0^2 + V$. The characteristic equation for the eigenvalue of the square mass operator is

$$\lambda^{-1} = \frac{1}{m_r}\langle\chi|G^V(M_{ps}^2)|\chi\rangle = \frac{1}{m_r}\int \mathrm{d}\vec{k}\int \mathrm{d}\vec{k'}\frac{g(M_0^2)}{\sqrt{A(k)}}\langle\vec{k}|G^V(M_{ps}^2)|\vec{k'}\rangle\frac{g(M_0'^2)}{\sqrt{A(k')}}. \tag{13}$$

We have not yet defined λ in eq. (13). To do that, we first recall the characteristic equation of the renormalized theory with the singular hyperfine interaction ($g(M_0^2) = 1$). The bare coupling constant is obtained from the value of the pion mass and substituted in the characteristic equation which gives the mass of the pseudoscalars. Then, the characteristic equation appears in a subtracted form, in which the divergence in the momentum integration is removed [8]:

$$\left[\frac{1}{m_r}\int \mathrm{d}\vec{k}\int \mathrm{d}\vec{k'}\frac{1}{\sqrt{A(k)}}\langle\vec{k}|G^V(M_\pi^2)|\vec{k'}\rangle\frac{1}{\sqrt{A(k')}}\right]_{(m_u,m_{\overline{u}})} - \left[\frac{1}{m_r}\int \mathrm{d}\vec{k}\int \mathrm{d}\vec{k'}\frac{1}{\sqrt{A(k)}}\langle\vec{k}|G^V(M_{ps}^2)|\vec{k'}\rangle\frac{1}{\sqrt{A(k')}}\right]_{(m_1,m_2)} = 0, \tag{14}$$

where $m_{u(\overline{u})}$ is the mass of the light constituent quark. Observe that the physical information contained in the pion wave function at short distances is carried to any other quark-antiquark system in eq. (14) by the operator

$$\mathcal{O}_\pi(M_\pi^2) := \left[\frac{1}{m_r}\frac{1}{\sqrt{A(\widehat{k})}}G^V(M_\pi^2)\frac{1}{\sqrt{A(\widehat{k})}}\right]_{(m_u,m_{\overline{u}})}, \tag{15}$$

which has its matrix element evaluated at the origin in (14). The hat indicates the operator quality.

In the case of the present regulated model we define for each meson a value of λ assuming that the form factor $g(M_0^2)$ selects the relevant momentum region of the interacting quarks, or the relevant region of virtuality of the quark-antiquark pair, within the particular meson. Thus, the matrix element of the operator $\mathcal{O}(M_\pi^2)$ should be taken between states defined by the function $g(M_0^2)$. Introducing the operator $\mathcal{O}_{ps}(M_{ps}^2)$ for a general pseudoscalar meson, which has expression analogous to eq. (15), one has

$$\mathcal{O}_{ps}(M_{ps}^2) := \left[\frac{1}{m_r}\frac{1}{\sqrt{A(\widehat{k})}}G^V(M_{ps}^2)\frac{1}{\sqrt{A(\widehat{k})}}\right]_{(m_1,m_2)}. \tag{16}$$

Then, using the operators defined in eqs. (15) and (16), it is reasonable to generalize eq. (14) to the following form:

$${}_{ps}\langle g|\mathcal{O}_\pi(M_\pi^2) - \mathcal{O}_{ps}(M_{ps}^2)|g\rangle_{ps} = 0, \tag{17}$$

where $\langle\vec{k}|g\rangle_{ps} := g(M_0^2)$ with $M_0 = \sqrt{k^2+m_1^2} + \sqrt{k^2+m_2^2}$. The strength of the short-range interaction for each pseudoscalar meson is determined by the pion mass and the regulator form factor according to

$$\lambda_{ps}^{-1} = {}_{ps}\langle g|\mathcal{O}_\pi(M_\pi^2)|g\rangle_{ps}. \tag{18}$$

The short-range part of the interaction parameterizes contributions from Fock components with high virtuality in the decomposition of the resolvent in eq. (1), which are important to bind strongly the quark-antiquark pair to form the pion. Otherwise, if one resorts only to the perturbative one-gluon exchange, the complex nonperturbative mechanism responsible for the pion formation as a Goldstone boson is washed out.

In the three-momentum basis eq. (17) reads

$$\int \mathrm{d}\vec{k} \int \mathrm{d}\vec{k}' g(M_0^2) \times \left(\left[\frac{1}{m_r} \frac{1}{\sqrt{A(k)}} \langle \vec{k}|G^V(M_\pi^2)|\vec{k}'\rangle \frac{1}{\sqrt{A(k')}} \right]_{(m_u, m_{\overline{u}})} - \left[\frac{1}{m_r} \frac{1}{\sqrt{A(k)}} \langle \vec{k}|G^V(M_{ps}^2)|\vec{k}'\rangle \frac{1}{\sqrt{A(k')}} \right]_{(m_1, m_2)} \right) \times g(M_0'^2) = 0, \quad (19)$$

where M_0^2 and $M_0'^2$ are computed for the quarks with masses m_1 and m_2.

In our calculation procedure, the resolvent is numerically obtained from

$$G^V(M_{ps}^2) = G_0(M_{ps}^2) + G_0(M_{ps}^2) T^V(M_{ps}^2) G_0(M_{ps}^2), \quad (20)$$

where the T-matrix is the solution of the Lippman-Schwinger equation:

$$T^V(M_{ps}^2) = V + V G_0(M_{ps}^2) T^V(M_{ps}^2), \quad (21)$$

where the free resolvent is $G_0(M_{ps}^2) = [M_{ps}^2 - M_0^2]^{-1}$. The detailed expressions can be found in ref. [8].

The valence component of the light-front wave function of the meson is the solution of eq. (2) given by eq. (12). By using eq. (20), we can write the valence wave function as

$$\psi(x, \vec{k}_\perp) = \frac{1}{\sqrt{x(1-x)}} \frac{G_{ps}}{M_{ps}^2 - M_0^2} \times \left[g(M_0^2) + \int \mathrm{d}\vec{k}' \sqrt{\frac{A(k)}{A(k')}} \langle \vec{k}|T^V(M_{ps}^2)|\vec{k}'\rangle g(M_0'^2) \right], \quad (22)$$

where the overall normalization factor of the $q\overline{q}$ Fock component of the meson wave function is G_{ps}. The three-momemtum is expressed in terms of the light-cone momentum with the transformation (4). The first term in eq. (22) dominates at large momentum if $g(M_0^2) = 1$ (corresponding to the asymptotic form), differently from this situation, when $g(M_0^2) \neq 1$, the two terms can compete even in the asymptotic region.

2.2 Constituent-quark masses and mass splittings

Within the present model, the low-lying vector mesons are weakly bound systems of constituent quarks while the pseudoscalars are strongly bound. Therefore in this model, the masses of the constituent quarks are obtained directly from the vector meson masses, as [13]

$$\begin{aligned} m_u &= \frac{1}{2} M_\rho = 384\,\mathrm{MeV}, \\ m_s &= M_{K^*} - \frac{1}{2} M_\rho = 508\,\mathrm{MeV}, \\ m_c &= M_{D^*} - \frac{1}{2} M_\rho = 1623\,\mathrm{MeV}, \\ m_b &= M_{B^*} - \frac{1}{2} M_\rho = 4941\,\mathrm{MeV}, \end{aligned} \quad (23)$$

where the masses of the vector mesons are 768 MeV, 892 MeV, 2007 MeV and 5325 MeV for the ρ, K^*, D^* and B^*, respectively [11]. The constituent masses for the up and down quarks are considered equal (we disregarded the small few MeV difference in the current up and down masses [11]). Using the value of the light-constituent-quark mass of 384 MeV and assuming that the effect of chiral symmetry breaking is about the same for each flavor, one gets an estimate of the current quark mass as $m_Q^{curr} = m_Q - m_u$ [13]. The current quark masses are estimated as $m_s^{curr} = 124\,\mathrm{MeV}$, $m_c^{curr} = 1239\,\mathrm{MeV}$ and $m_b^{curr} = 4557\,\mathrm{MeV}$ consistent with ref. [11].

In our model, the binding energy of the constituent quarks in the pseudoscalar mesons, is interpreted as the ${}^1S_0$-${}^3S_1$ meson mass splitting, and thus a quantity directly related to data. The binding energy is simply $B_{ps} = M_v - M_{ps}$ defined to be positive. The experimental values for the ground-state quantities show evidence for a strong correlation of B_{ps} and M_{ps} qualitatively reproduced by the renormalized model with singular interaction [8]. We will see in sect. 4 that eq. (17) also provides a reasonable description of the mass splitting.

3 Electromagnetic form factor and weak-decay constant

To obtain the electromagnetic form factor and the pseudoscalar decay constant, we follow the suggestion of refs. [25,29]. To construct such observables, one describe the coupling of the pseudoscalar meson field ($\Phi_{ps}(\vec{x})$) to the quark fields ($q_1(\vec{x})$ and $q_2(\vec{x})$) by an effective Lagrangian density with a pseudoscalar coupling of the quark fields:

$$\mathcal{L}_{eff}(\vec{x}) = -i\Gamma_{ps} \Phi_{ps}(\vec{x})\ \overline{q}_1(\vec{x}) \gamma^5 q_2(\vec{x}) + \mathrm{h.c.}, \quad (24)$$

where Γ_{ps} is a constant vertex. After the integration in the minus momentum component of the momentum integration of the one-loop amplitudes that define the electromagnetic form factor and weak-decay constant, the asymptotic form of the wave function is substituted by the valence component of the model wave function. The integration in the minus momentum component eliminates the relative time between the quarks in the intermediate states [28].

3.1 Form factor of pseudoscalar mesons

The pseudoscalar meson electromagnetic form factor is obtained from the impulse approximation of the plus com-

ponent of the current ($j^+ = j^0 + j^3$) in the Breit frame with momentum transfer $q^+ = 0$ and $q^2 = -\vec{q}^2$ satisfying the Drell-Yan condition. The general structure of the $q\overline{q}$ bound state forming the meson comes from the pseudoscalar coupling (24). We use such spin structure in the computation of the photo-absorption amplitude in the impulse approximation (represented by a Feynman triangle diagram), which is written as

$$(p_\pi^\mu + p_\pi'^\mu)F_{ps}(q^2) = i\Gamma_{ps}^2 e_1 N_c \times \int \frac{\mathrm{d}^4k}{(2\pi)^4}\mathrm{tr}\Big[\frac{\not k + m_2}{k^2 - m_2^2 + i\varepsilon}\gamma^5\frac{\not k - \not p' + m_1}{(k-p')^2 - m_1^2 + i\varepsilon} \times\gamma^\mu\frac{\not k - \not p + m_1}{(k-p)^2 - m_1^2 + i\varepsilon}\gamma^5\Big] + [1 \leftrightarrow 2], \quad (25)$$

where $F_{ps}(q^2)$ is the electromagnetic form factor and e_i is the quark charge. The meson momentum in the initial and final states are defined by $p^0 = p'^0$ and $\vec{p'}_\perp = -\vec{p}_\perp = \frac{\vec{q}_\perp}{2}$. $N_c = 3$ is the number of colors.

The choice of the plus component of the current is adequate in the case of pseudoscalars mesons because after the integration over $k^- = k^0 - k^3$ the suppression of the pair diagram is maximal for this component in the frame where $q^+ = 0$ and just the wave function components contribute to the form factor [25,29–31]. In our model, only the valence component is considered. Although we compute the integration in the minus momentum component assuming a constant vertex, one can identify in the expression how the valence component of the wave function correspondent to the non-constant vertex of eq. (22) should be introduced. As the details of this derivation is by now standard, we present directly the final result:

$$F_{ps}(q^2) = e_1\frac{N_c}{(2\pi)^3}\int_0^1\frac{\mathrm{d}x}{1-x}\int \mathrm{d}^2k_\perp \times\Big[2m_1m_2 - 2m_1^2 + k_{1on}^- p^+ + k^+(m_1-m_2)^2 - k^+\vec{q}_\perp^{\,2}\Big] \times\psi_{ps}(x,\vec{K}_\perp)\psi_{ps}(x,\vec{K'}_\perp) + [1\leftrightarrow 2], \quad (26)$$

where the momentum fraction is $x = k^+/p^+$ and $k_{1on}^- = (\vec{k}_\perp^{\,2} + m_1^2)/k^+$. The quark transverse momentum in the meson rest frame is given by

$$\vec{K}_\perp = \vec{k}_\perp + x\frac{\vec{q}_\perp}{2} \quad (27)$$

and $\vec{K'}_\perp = \vec{K}_\perp - x\vec{q}_\perp$. The expression for the form the factor gives the standard Drell-Yan formula once the bound-state wave function of the constant vertex model (asymptotic form) is recognized

$$\psi^\infty(x,\vec{K}_\perp) = \frac{G_{ps}}{\sqrt{x(1-x)}\,(m_\pi^2 - M_0^2)}\,, \quad (28)$$

which is the first term in eq. (22) for $g(M_0^2) = 1$. The second term in (22) comes from the Coulomb-like interaction. The other factors in eq. (26) compose the Melosh rotations of the individual spin wave function of the quarks.

The size of the meson is closely related to the square-root mean square charge radius which is calculated as

$$\sqrt{\langle r_{ps}^2\rangle} = \Big[6\frac{\mathrm{d}}{\mathrm{d}q^2}F_{ps}(q^2)|_{q^2=0}\Big]^{\frac{1}{2}}.$$

In sect. 4 we adjust the regularization parameter (see eq. (35)) by fitting the pion charge radius, $\sqrt{\langle r_\pi^2\rangle}$, which has an experimental value of $0.67 \pm 0.02\,\mathrm{fm}$ [32]. The charge radius from eq. (26) in the soft-pion limit ($M_\pi = 0$) using the asymptotic wave function (28), with $\Gamma_\pi = \sqrt{2}m_{u(d)}/f_\pi$ from the Goldberger-Treiman [33] relation at the quark level, results in the well-known expression $\sqrt{\langle r_\pi^2\rangle} = \sqrt{3}/(2\pi f_\pi)$ from refs. [23,24]. In this case, also the form factor (26) for $q^2 = 0$ reduces to the expression for f_π as given in [25]. We observe that our model, for $\alpha = 0$, $g(M_0^2) = 1$ and $M_\pi = 0$ recovers the soft-pion result, *i.e.* $\sqrt{\langle r_\pi^2\rangle} = 0.58\,\mathrm{fm}$.

3.2 Weak-decay constant

The leptonic weak-decay constant of the pseudoscalar meson (f_{ps}) is a physical quantity that depends directly on the probability to find the quark-antiquark Fock state component in the meson wave function [3]. Also, f_{ps} depends on the short-range physics carried by the wave function when the quark and antiquark are close.

The meson weak-decay constant is calculated from the matrix element of the axial current $A^\mu(0)$ between the vacuum state $|0\rangle$, and the meson state $|p\rangle_{ps}$ with four-momentum p [11]:

$$\langle 0 \mid A^\mu(0) \mid p\rangle_{ps} = \imath\sqrt{2}f_{ps}p^\mu, \quad (29)$$

where $A^\mu(\vec{x}) = \imath\overline{q}(\vec{x})\gamma^\mu\gamma^5 q(\vec{x})$.

The matrix element of the plus component of the axial current is derived from the pseudoscalar Lagrangian (24), and it is expressed by a one-loop diagram, which is given by

$$\imath\sqrt{2}M_{ps}f_{ps} = N_c\Gamma_{ps} \times\int\frac{\mathrm{d}^4k}{(2\pi)^4}\frac{Tr\left[\gamma^+\gamma^5(\not k - \not p + m_2)\gamma^5(\not k + m_1)\right]}{((k-p)^2 - m_2^2 + i\varepsilon)(k^2 - m_1^2 + i\varepsilon)}\,, \quad (30)$$

the plus component is used to eliminate the instantaneous terms of the Dirac propagator.

By integration of eq. (30) over k^-, one obtains the expression of f_{ps} suitable for the introduction of the meson light-front wave function. So, performing the Dirac algebra and separating the poles in the k^--plane and integrating, one gets

$$f_{ps} = -\frac{\sqrt{2}}{8\pi^3}N_c\int_0^1\frac{\mathrm{d}x}{x(1-x)}\left((1-x)m_1 + xm_2\right) \times\int\mathrm{d}^2k_\perp\frac{\Gamma_{ps}}{M_{ps}^2 - M_0^2}\,, \quad (31)$$

where the quark 1 has momentum fraction x. This expression is written in the meson rest-frame and we have used the momentum fraction $x = k^+/p^+$. The free square mass is defined in eq. (3). Note that this expression has a log-type divergence in the transverse momentum integration which was discussed in ref. [15] and parameterized in terms of f_π.

One can write eq. (31) in terms of the valence component of the pseudoscalar meson wave function from eq. (22), as

$$f_{ps} = \frac{\sqrt{2}}{8\pi^3} N_c \int_0^1 \frac{\mathrm{d}x}{\sqrt{x(1-x)}} \left((1-x)m_1 + xm_2\right) \times \int \mathrm{d}^2 k_\perp \psi(x, \vec{k}_\perp), \tag{32}$$

with x being the momentum fraction of quark 1. It is enough to choose $g(M_0^2)$ decaying as $M_0^{-\eta}$ for any $\eta > 0$, to make f_{ps} finite.

In the particular case of $g(M_0^2) = 1$ the meson wave function, eq. (22), for large transverse momentum behaves as the asymptotic wave function, which decreases slowly as $p_\perp^{-2}$ implying logarithmic divergences in the transverse momentum integrations of the weak-decay constant and form factor. In refs. [14] and [15], the log-type divergent factors in the pseudoscalar decay constants were parameterized in terms of f_π and the sum of the constituent-quark masses, which in the QCD-inspired model [8] could be identified with the ground-state vector meson mass. Therefore, one has

$$f_{ps} = \text{const} \int_0^1 \mathrm{d}x \left((1-x)m_2 + xm_1\right), \tag{33}$$

and $f_{ps} \propto m_1 + m_2$ [14]. In our model $m_1 + m_2$ is the vector meson mass, and then as suggested by ref. [15], the decay constant scales as

$$\frac{f_{ps}}{f_\pi} = \frac{M_v}{M_\rho}, \tag{34}$$

which approximates the existing data up to the kaon and D mesons but is not supported by relativistic constituent-quark potential models and lattice QCD calculations, as we have discussed in the introduction. The use of the separable regulator in the model brings this consistency. We will return to this discussion in the next section.

4 Discussion of the numerical results and conclusion

The present QCD-inspired model for the effective square mass operator acting only on the valence component of the meson wave function, eq. (2), has the canonical number of parameters (the quark masses and α) plus two, when we choose the regulator form factor as

$$g^{(a)}(M_0) = \frac{1}{\beta^{(a)} + M_0^2} \text{ or } g^{(b)}(M_0) = \frac{1}{M_0^2} + \left(\frac{\beta^{(b)}}{M_0^2}\right)^2. \tag{35}$$

The form factor (a) for equal-mass quarks is the familiar Yukawa form in coordinate space. The other choice just contains the first two terms of a Taylor expansion of $g^{(a)}$ for large M_0^2. In the limit of $\beta^{(a)} \to \infty$ the model with form factor $g^{(a)}$ reduces to the renormalized model of ref. [8], while by construction the form factor $g^{(b)}$ is qualitatively different as it does not allow to match that model. Nonetheless, for finite β's, as we will see from our numerical calculations, both form factors produce practically the same results.

The parameters β and the strength of the separable interaction λ_{ps}, eq. (18), are adjusted to reproduce the experimental pion charge radius $0.67 \pm 0.02\,\mathrm{fm}$ [32] and mass, $M_\pi = 140\,\mathrm{MeV}$, for each form factor $g^{(a)}$ and $g^{(b)}$ independently. We use a light-quark constituent mass of 384 MeV (see eq. (23)) and f_π results to be 110 MeV for both separable interactions (see table 1). The somewhat higher value for f_π, compared to the experimental value of $92.4 \pm .07 \pm 0.25$ [11], is a common shortcoming of light-front models of the pion when the valence wave function is normalized to one [29,31]. The valence component appears to have a probability of about 70% (see also [29,31]) which brings the model results for f_π to 92 MeV. In the case of $\alpha = 0.5$, the resulting parameters for the form factors are $\beta^{(a)} = -(634.5\,\mathrm{MeV})^2$ and $\beta^{(b)} = (1171\,\mathrm{MeV})^2$.

Let us note that the known nonperturbative dynamics of QCD is parameterized by the quark and gluon condensates. The quark condensate is implicitly accounted by the model through the values of the pion mass and weak-decay constant by recalling the Gell-Mann, Oakes and Renner relation: $f_\pi^2 M_\pi^2 = -(m_u^{curr} + m_d^{curr})\langle \bar{u}u + \bar{d}d\rangle/2$ [34]. The role of the gluon condensate within the model is less obvious, presumably it is related to all parameters and with the constituent-quark masses. The other important parameter is $\Lambda_{QCD} \sim 0.2\,\mathrm{GeV}$ [11] which sets the QCD scale for the running coupling constant. Our model is fitted to a reasonable average hadronic scale of $\mu \sim 1\,\mathrm{GeV}$ which gives $\alpha \sim 0.4$ (compared to 0.5), from the lowest-order evaluation of the running coupling constant $\alpha = 12\pi/((33 - 2n_f)\log(\mu^2/\Lambda_{QCD}^2))$ [33].

It would be plausible to use a running coupling constant as a function of the momentum transfer in eq. (2). However, as we are also fitting the parameters of the hyperfine interaction to fix the pion mass and radius and we will be bound to introduce a momentum cut-off for which, below it, for example, a fixed value will be used, we believe that, after all, the results will be not strongly dependent on the running coupling constant.

In fig. 1 we show the results for the $^3S_1$-$^1S_0$ meson mass splitting, the binding energy B_{ps}, as a function of the pseudoscalar meson mass. We choose $\alpha = 0.5$ and the form factor regulator $g^{(a)}$ (the differences between the masses obtained with the two form of regulators are less than 1 MeV). In the figure we see the dependence of the mass splitting of $q\overline{Q}$ mesons on the pseudoscalar mass, obtained by the the variation of m_Q, while m_q is fixed at the values of 384 MeV (solid line), 508 MeV (dashed line) and 1623 MeV (dotted line). In this way, we simulate the families of mesons with an up or down, a strange and charm

Table 1. Results for the pseudoscalar weak-decay constants f_{ps} compared with others calculations and experimental data. The calculations of f_{ps} for $\alpha = 0.5$ with regulator form factors $g^{(a)}(M_0) = \left(-(634.5)^2 + M_0^2\right)^{-1}$ and $g^{(b)}(M_0) = 1/M_0^2 + \left(1171/M_0^2\right)^2$ are given in the second and third columns, respectively. In the fourth column the global estimates from lattice QCD results [18] are shown. The experimental values for the decay constants [11,35,36] are shown in the fifth column. In the last two columns it is given the masses of the pseudoscalars obtained with model (a) and the corresponding experimental values [11]. The masses obtained with model (b) (not shown in the table) and with model (a) differ by less than 1 MeV. The decay constants and masses are all given in MeV. (The experimental errors in the masses are small excepting for B_c^+ which has a large error.)

$q\overline{q}$	$f_{ps}^{(a)}$	$f_{ps}^{(b)}$	f_{ps}^{Latt} [18]	f_{ps}^{exp}	$M_{ps}^{(a)}$	M_{ps}^{exp} [11]
$\pi^+(u\overline{d})$	110	110	–	$92.4 \pm .07 \pm 0.25$ [11]	140	140
$K^+(u\overline{s})$	126	121	–	$113.0 \pm 1.0 \pm 0.31$ [11]	490	494
$D^+(c\overline{d})$	164	159	$166 \pm 8 \pm 13^{+\ 0}_{-15}(\chi\log)$	$212^{+127+56}_{-106-28}$ [11] $202 \pm 41 \pm 17$ [35] $262^{+91}_{-84} \pm 18$ [36]	1861	1869
$D_s^+(c\overline{s})$	184	178	$187 \pm 8 \pm 15$	188 ± 23 [11]	1961	1969
$B^+(u\overline{b})$	118	117	$135 \pm 16^{+\ 0}_{-15}(\chi\log)$	–	5242	5279
$B_s^0(s\overline{b})$	154	154	156 ± 18	–	5342	5370
$B_c^+(c\overline{b})$	375	375	–	–	6257	6400 ± 400

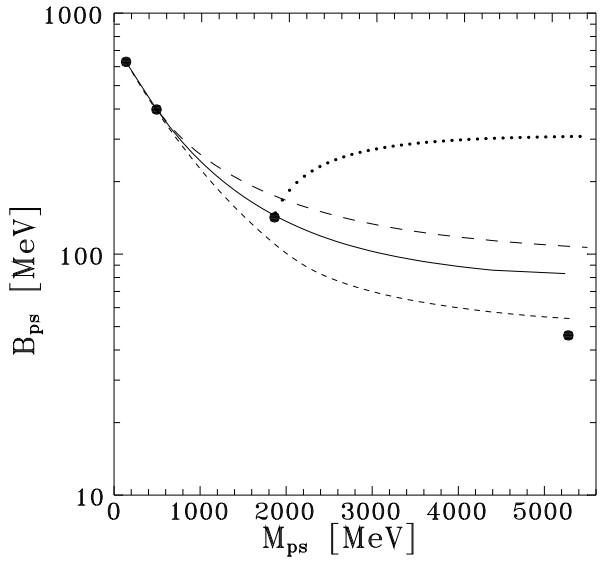

Fig. 1. $^3S_1$-$^1S_0$ meson mass splitting (B_{ps}) as a function of the pseudoscalar meson mass. The calculations for $q\overline{Q}$ mesons are performed, with the regulator form factor $g^{(a)}(M_0) = (\beta^{(a)} + M_0^2)^{-1}$ ($\beta^{(a)} = -(634.5\,\mathrm{MeV})^2$ and $\alpha = 0.5$), by varying the mass m_Q with m_q fixed at 384 MeV (solid line), 508 MeV (dashed line) and 1623 MeV (dotted line). The results of the renormalized model from ref. [8] with $\alpha = 0.5$ and fixed $m_q = 384$ MeV are shown by the short-dashed line. The experimental values of the mass splitting for ρ-π, K^*-$K^\pm$, D^{*0}-D^0 and B^*-$B^\pm$ [11] are given by the full circles.

quarks and a distinct one which has mass m_Q. First, we compare the results of the present regularized model with the previous results of the renormalized model [8] found for $m_q = 384$ MeV and $\alpha = 0.5$. In this case, the regularization increases B_{ps} as seen in the figure. The regularization procedure naturally softens the attractive part of interaction at short distances, which should be compensated by an effective increase of the strength of the separable interaction to keep the pion still strongly bound at its physical mass. The increase of the strength is reflected in the increase of binding, as seen in the figure. Still the trend of the experimental values of the mass splitting for ρ-π, K^*-$K^\pm$, D^{*0}-D^0 and B^*-$B^\pm$ [11] is found.

The results of the mass splitting for mesons containing at least one strange meson (dashed line in fig. 1) exhibit the same qualitative behavior found for mesons with an up or down quark, *i.e.*, the mass splitting decreases with the rise of the mass of the heavy quark. This should be the case since the masses of the constituents, up-down and strange, are very much similar, with an expected increase in the mass splitting when the up-down quark is exchanged with one strange quark which is heavier. By rising the mass of one of the constituents for mesons with charm (dotted line of fig. 1) the splitting increases, because the quarks become spatially closer and the binding is expected to rise as in nonrelativistic potential models. Also, as expected, the saturation of the binding energy appears for large masses.

In fig. 2 we show the weak-decay constant as a function of the intensity parameter α of the Coulomb-like interaction for different mesons. The calculations are performed with the regulator form factor $g^{(a)}(M_0) = (b + M_0^2)^{-1}$ with the parameter b adjusted for each given α between 0.1 and 0.5 in order to reproduce $f_\pi = 110$ MeV. The kaon weak-decay constant varies less than one MeV in this interval keeping the value 126 MeV (see table 1). We show in the figure only results for D^+ (solid line), D_s^+ (dashed line), B^+ (solid line with dots) and B_c^+ (dashed line with dots). The decay constants rise with α, as the $q\overline{Q}$ systems become more bound and compact due to increase in the Coulomb-like interaction. The effect is particularly dramatic for the heavier mesons B^+ and B_c^+ as

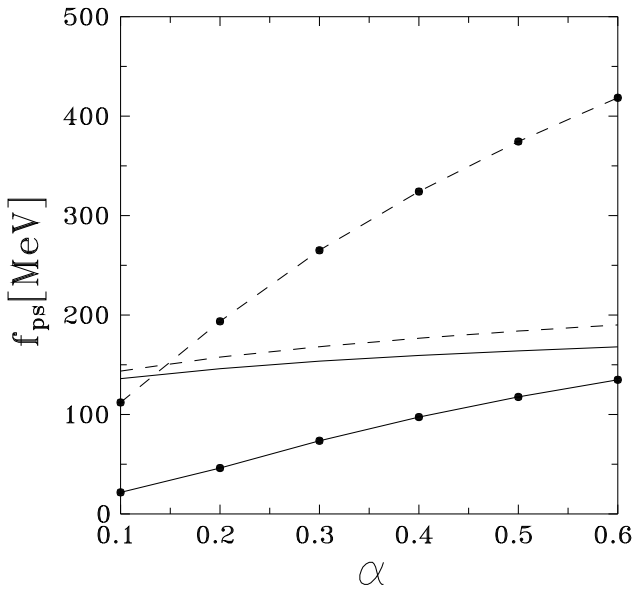

Fig. 2. Weak-decay constant as a function of the intensity parameter α of the Coulomb-like interaction for different mesons. The calculations are performed with the regulator form factor $g^{(a)}(M_0) = (\beta^{(a)} + M_0^2)^{-1}$. The parameter $\beta^{(a)}$ is adjusted to fit $f_\pi = 110\,\mathrm{MeV}$ for each given α. Results for D^+ (solid line), D_s^+ (dashed line), B^+ (solid line with dots) and B_c^+ (dashed line with dots).

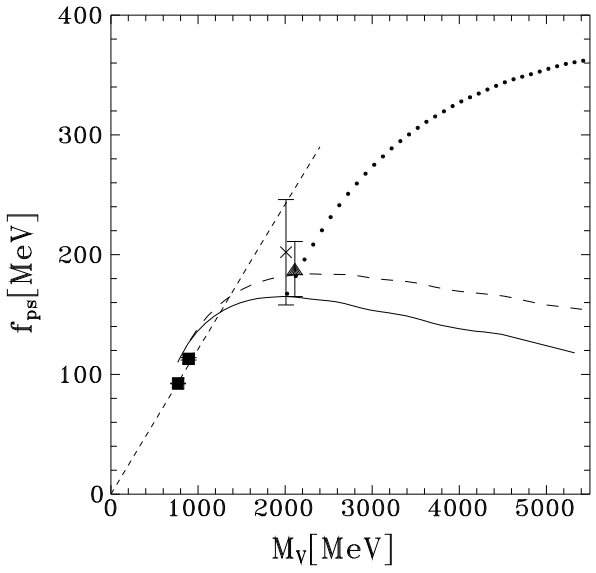

Fig. 3. Pseudoscalar meson weak-decay constant as a function of the vector meson mass. The calculations for $q\overline{Q}$ mesons are performed with the regulator form factor $g^{(a)}(M_0) = (\beta^{(a)}+M_0^2)^{-1}$ ($\beta^{(a)} = -(634.5\,\mathrm{MeV})^2$ and $\alpha = 0.5$), by varying the mass m_Q with m_q fixed at 384 MeV (solid line), 508 MeV (dashed line) and 1623 MeV (dotted line). The short-dashed line gives f_{ps} obtained from eq. (34). The experimental values are given by the full squares [11] (f_π and f_K in order of increasing values); the cross [35] (f_{D^+}) and the full triangle [11] ($f_{D_s^+}$).

could be anticipated thinking within a nonrelativistic potential model, where the probability to found the quarks at the origin should increase when the attractive force is strengthened.

The pseudoscalar meson weak-decay constant as a function of the vector meson mass is shown in fig. 3 as suggested by eq. (34). The calculations were performed with the regulator form factor (a) and $\alpha = 0.5$. In the figure we see dependence of f_{ps} for $q\overline{Q}$ mesons with the vector meson mass, obtained through the variation of m_Q, while m_q is fixed at the values of 384 MeV (solid line), 508 MeV (dashed line) and 1623 MeV (dotted line). Although the naive model of eq. (34), which presents a linear increase of f_{ps} with M_v, gives some qualitative insight into the data, it fails to describe the saturation and decrease of the results of the regulated model, which as expected has a f_{ps} decreasing with the mass of the meson. The data for D_s^+ is indeed below the linear curve and consistent with the dashed curve calculated with the regulated model for $s\overline{Q}$ pseudoscalars. There are several experimental values for f_{D^+} obtained by different collaborations as quoted in table 1. In figs. 3 and 4 we just indicate the experimental result from [35].

The values of f_{ps} for mesons with one charm quark (dotted line in fig. 3) increase with M_v, as the system becomes more compact up to the point that f_{ps} saturates for $M_v \gg m_c = 1623\,\mathrm{MeV}$ (the probability density at the origin does not change anymore) while the expected $1/\sqrt{M_Q}$-dependence dominates for large values of M_v.

In fig. 4, the weak-decay constant as a function of the pseudoscalar meson mass obtained in our regulated model with form factor (a) and $\alpha = 0.5$ is compared to the recent global average of lattice QCD results [18]. The short-dashed line gives a least-square fit to the experimental values of f_π and f_K together with the lattice estimates for D^+ and B^+ [16] given by $f_{ps}^2 = (0.0065 + 0.014 M_{ps})/(1 + 0.055 M_{ps} + 0.15 M_{ps}^2)\,\mathrm{GeV}^2$ as given in ref. [12], where the $1/\sqrt{M_{ps}}$ behavior for large masses is built in. The results for $u\overline{Q}$ pseudoscalars are in qualitatively agreement with that fit. Our calculations for $u\overline{Q}$ and $s\overline{Q}$ pseudoscalar mesons are in a good consistency with the global lattice averages of the weak-decay constants, as seen by comparing the solid line with the full circles for $u\overline{Q}$ mesons and the dashed line with the full stars for $s\overline{Q}$ mesons.

To close our study of the present regulated model in figs. 5, 6 and 7 we show results for the pion and kaon electromagnetic form factors using $\alpha = 0.5$ with the model regulated with form factor (a). The pion mean-square radius is reasonable fitted as well as the form factor up to about $4\,[\mathrm{GeV}/c]^2$ as shown in fig. 5. The experimental values for kaon form factor [21,22] present large errors and do not allow a definite conclusion as seen in fig. 6. For completeness, we present the kaon form factor calculation

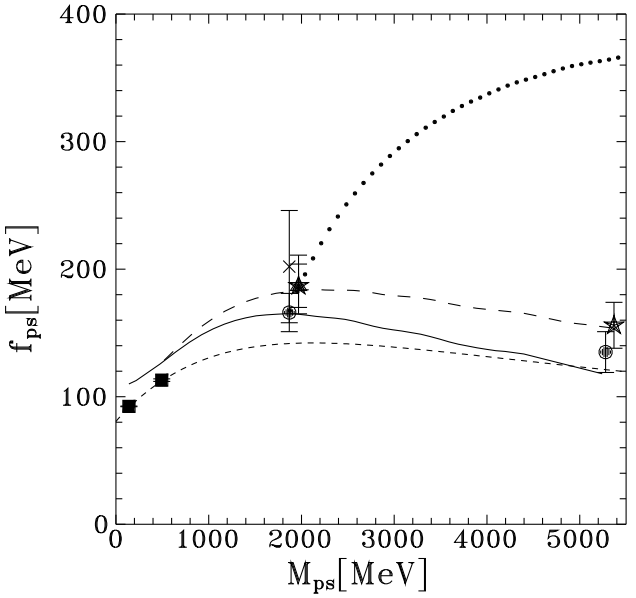

Fig. 4. Pseudoscalar meson weak-decay constant as a function of the pseudoscalar meson mass. The calculations for $q\overline{Q}$ mesons are performed with the regulator form factor $g^{(a)}(M_0) = (\beta^{(a)} + M_0^2)^{-1}$ ($\beta^{(a)} = -(634.5\,\mathrm{MeV})^2$ and $\alpha = 0.5$), by varying the mass m_Q with m_q fixed at 384 MeV (solid line), 508 MeV (dashed line) and 1623 MeV (dotted line). The global estimates of lattice QCD results [18] for f_{D^+} and f_{B^+} are given by the full circles and for $f_{D_s^+}$ and $f_{B_s^0}$ by the full stars. The short-dashed line gives a least-square fit to the experimental values of f_π and f_K together with the lattice estimates for D^+ and B^+ [16] as performed in ref. [12]. The experimental values are given by the full squares [11] (f_π and f_K in order of increasing values); the cross [35] (f_{D^+}) and the full triangle [11] ($f_{D_s^+}$).

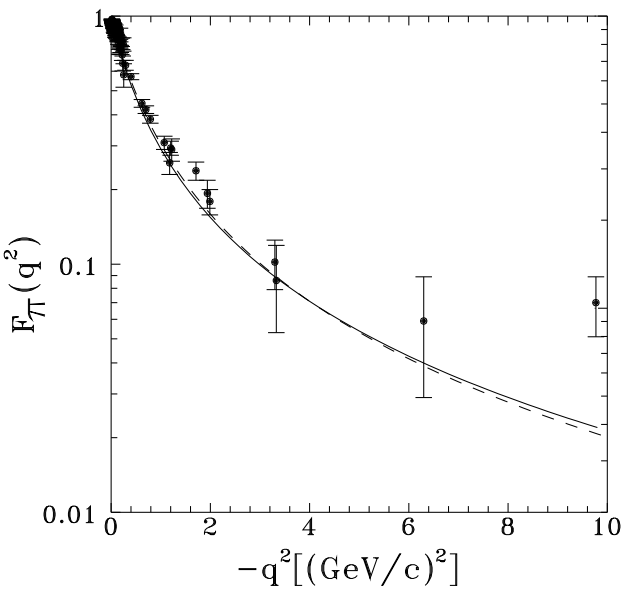

Fig. 5. Pion electromagnetic form factor. The results of the calculations performed with $\alpha = 0.5$ considering the regulator form factors $g^{(a)}(M_0) = (-(634.5)^2 + M_0^2)^{-1}$ and $g^{(b)}(M_0) = 1/M_0^2 + (1171/M_0^2)^2$ are given by the solid and dashed lines, respectively. The experimental data are from ref. [20].

up to 10 $[\mathrm{GeV}/c]^2$. We also compare with the calculations with the form factor (b), and we do not observe a strong model dependence below 4 $[\mathrm{GeV}/c]^2$.

In table 1, we present the results for the pseudoscalar weak-decay constants f_{ps} for π, K, D^+, D_s^+, B^+, B_s^0 and B_c^+ compared to global estimates of lattice QCD results and experimental data. The consistence with lattice results indicates that the regularized model is able to parameterize the QCD physics at short distances, in the ground state of the pseudoscalar mesons, quite reasonably. The pseudoscalar masses are underestimated for the heavy mesons, as already seen in fig. 1, although the saturation behavior of the mass splitting that the data indicates is verified by the calculation. This problem can be overcome by the introduction of confinement in the model [27,37].

In summary, we have shown that the suggested separable form to regulate the singular interaction in the square mass operator provides a reasonable description of the mass splitting between $^3S_1$ and $^1S_0$ meson ground states, the weak-decay constants as found in a recent global average of lattice results [18] and the pion form factor up to 4 $[\mathrm{GeV}/c]^2$. The main point here is that the model can

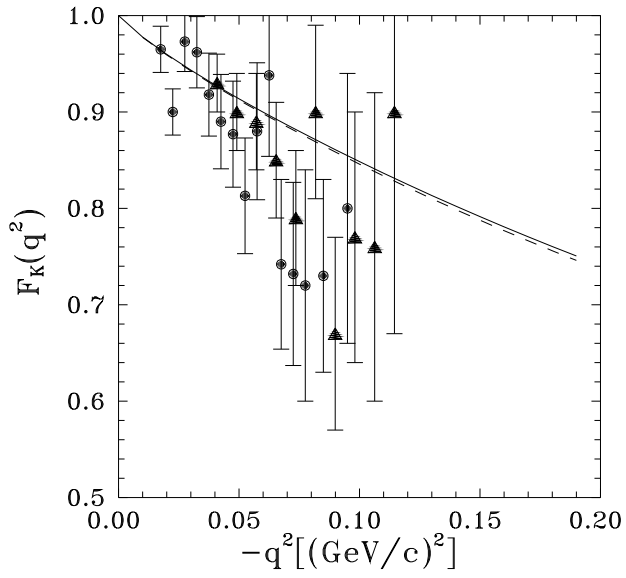

Fig. 6. Kaon electromagnetic form factor. The results of the calculations performed with $\alpha = 0.5$ considering the regulator form factors $g^{(a)}(M_0) = (-(634.5)^2 + M_0^2)^{-1}$ and $g^{(b)}(M_0) = 1/M_0^2 + (1171/M_0^2)^2$ are given by the solid and dashed lines, respectively. The experimental data from ref. [21] are shown by the full triangles and those from ref. [22] by the full circles.

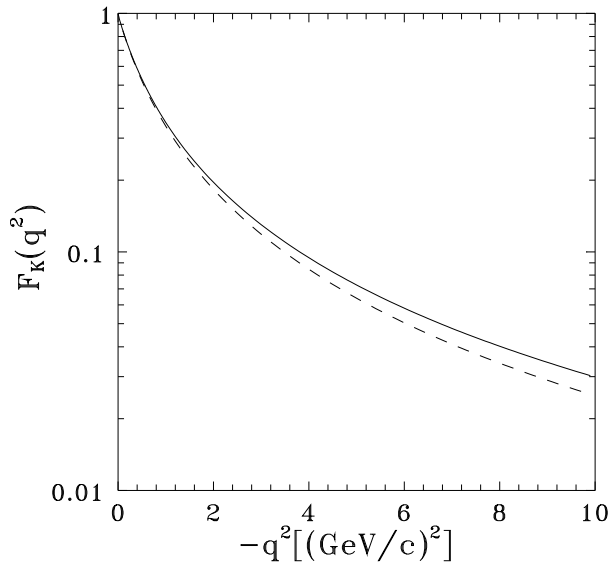

Fig. 7. Kaon electromagnetic form factor up to $10\,(\mathrm{GeV}/c)^2$. The results of the calculations performed with $\alpha = 0.5$ considering the regulator form factors $g^{(a)}(M_0) = (-(634.5)^2 + M_0^2)^{-1}$ and $g^{(b)}(M_0) = 1/M_0^2 + (1171/M_0^2)^2$ are given by the solid and dashed lines, respectively.

describe the mass dependence of the weak-decay constant, revealing that the physics in this observable is dominated by the mass of the meson itself, through the quark masses and binding. The effective square mass operator acting on the valence component of the light-front meson wave function is again tested and proved to reasonably parameterize the dynamics of the constituents at short distances. The present version of the model does not have explicit confining interaction, therefore it is not able to account for the spectra. A more sophisticated version of the model that includes confinement was shown to describe the meson spectrum [27] and the pion form factor in the space and time-like regions [38], can also be used in the future in a regularized form to allow the calculation of the pseudoscalar decay constants.

We thank CNPq (Conselho Nacional de Desenvolvimento Cientí fico e Tecnológico) and FAPESP (Fundação de Amparo a Pesquisa do Estado de São Paulo) of Brazil for financial support.

References

1. M.V. Terentev, Sov. J. Nucl. Phys. **24**, 106 (1976); L.A. Kondratyuk, M.V. Terentev, Sov. J. Nucl. Phys. **31**, 561 (1976).
2. V.B. Berestesky, M.V. Terentev, Sov. J. Nucl. Phys. **24**, 547 (1976); **25**, 347 (1977).
3. S.J. Brodsky, H.C. Pauli, S.S. Pinsky, Phys. Rep. **301**, 299 (1998).
4. H.C. Pauli, Nucl. Phys. B (Proc. Suppl.) **90**, 259 (2000).
5. H.C. Pauli, Nucl. Phys. B (Proc. Suppl.) **90**, 154 (2000).
6. H.C. Pauli, Eur. Phys. J. C **7**, 289 (1998).
7. H.C. Pauli, *DLCQ and the effective interactions in hadrons*, in *New Directions in Quantum Chromodynamics*, edited by C.R. Ji, D.P. Min (AIP, 1999) pp. 80-139.
8. T. Frederico, H.-C. Pauli, Phys. Rev. D **64**, 054007 (2001); T. Frederico, M. Frewer, H.-C. Pauli, Nucl. Phys. B (Proc. Suppl.) **108**, 234 (2002).
9. S. Capstick, S. Godfrey, Phys. Rev. D **41**, 2856 (1990).
10. W. Jaus, Phys. Rev. D **53**, 1349 (1996).
11. Particle Data Group (S. Eidelman *et al.*), Phys. Lett. B **592**, 1 (2004) (URL: `http://pdg.lbl.gov`).
12. C.D. Roberts, *Unifying aspects of light- and heavy systems*, ArXiv:nucl-th/0304050.
13. E.F. Suisso, J.P.B.C. de Melo, T. Frederico, Phys. Rev. D **65**, 094009 (2002).
14. S.S. Gershtein, M. Yu. Khlopov, JETP Lett. **23**, 338 (1976); M. Yu Khlopov, Sov. J. Nucl. Phys. **28**, 483 (1978).
15. L.A.M. Salcedo, J.P.B.C. de Melo, D. Hadjmichef, T. Frederico, Braz. J. Phys. **34**, 297 (2004).
16. J.M. Flynn, C.T. Sachrajda, Adv. Ser. Direct. High Energy Phys. **15**, 402 (1998).
17. C. McNeile, *Heavy quarks on the lattice*, hep-lat/0210026.
18. H. Wittig, *Status of lattice calculations of B-meson decays and mixing*, hep-ph/0310329.
19. M.A. Ivanov, Yu. L. Kalinovsky, P. Maris, C.D. Roberts, Phys. Lett. B **416**, 29 (1998).
20. R. Baldini *et al.*, Eur. Phys. J. C **11**, 709 (1999); Nucl. Phys. A **666-667**, 3 (2000).
21. E.B. Dally *et al.*, Phys. Rev. Lett. **45**, 232 (1980).
22. S.R. Amendolia *et al.*, Phys. Lett. B **178**, 435 (1986).
23. S.B. Gerasimov, Sov. J. Nucl. Phys. **29**, 259 (1978); **32**, 156 (1980)(E).
24. R. Tarrach, Z. Phys. C **2**, 221 (1979).
25. T. Frederico, G.A. Miller, Phys. Rev. D **45**, 4207 (1992).
26. H.-C. Pauli, Nucl. Phys. B (Proc. Suppl.) **108**, 273 (2002); M. Frewer, T. Frederico, H.-C. Pauli, Nucl. Phys. B (Proc. Suppl.) **108**, 249 (2002).
27. T. Frederico, H.-C. Pauli, S.-G. Zhou, Phys. Rev. D **66**, 054007; 116011 (2002).
28. J.H.O. Sales, T. Frederico, B.V. Carlson, P.U. Sauer, Phys. Rev. C **61**, 044003 (2000); **63**, 064003 (2001).
29. T. Frederico, G.A. Miller, Phys. Rev. D **50**, 210 (1994).
30. J.P.B.C. de Melo, H.W. Naus, T. Frederico, Phys. Rev. C **59**, 2278 (1999).
31. J.P.B.C. de Melo, T. Frederico, E. Pace, G. Salmè, Nucl. Phys. A **707**, 399 (2002).
32. S.R. Amendolia *et al.*, Phys. Lett. B **178**, 116 (1986).
33. C. Itzykson, J.B. Zuber, *Quantum Field Theory* (McGraw-Hill, 1980).
34. M. Gell-Mann, M.R. Oakes, B. Renner, Phys. Rev. **175**, 2195 (1968).
35. CLEO Collaboration (G. Bonvicini *et al.*), Phy. Rev. D **70**, 112004 (2004).
36. BES Collaboration (M. Ablikim *et al.*), Phys. Lett. B **610**, 183 (2005).
37. M.G.C.L. Hoinacki, W.R.B. de Araújo, T. Frederico, Braz. J. Phys. **35**, 865 (2005).
38. J.P.B.C. de Melo, T. Frederico, E. Pace, G. Salmè, Phys. Lett. B **581**, 75 (2004).